

Seleno groups control the energy-level alignment between conjugated organic molecules and metals

Jens Niederhausen,¹ Steffen Duhm,^{2,3} Georg Heimel,¹ Christoph Bürker,⁴ Qian Xin,^{2,5} Andreas Wilke,¹ Antje Vollmer,⁶ Frank Schreiber,⁴ Satoshi Kera,² Jürgen P. Rabe,¹ Nobuo Ueno,² and Norbert Koch^{1,6}

¹*Institut für Physik, Humboldt-Universität zu Berlin, 12489 Berlin, Germany*

²*Graduate School of Advanced Integration Science, Chiba University, Chiba 263-8522, Japan*

³*Institute of Functional Nano and Soft Materials (FUNSOM), Soochow University, Suzhou 215123, People's Republic of China*

⁴*Institut für Angewandte Physik, Universität Tübingen, 72076 Tübingen, Germany*

⁵*School of Physics, Shandong University, 27 Shanda Nanlu, Jinan 250100, People's Republic of China*

⁶*Helmholtz-Zentrum Berlin für Materialien und Energie GmbH, BESSY II, 12489 Berlin, Germany*

(Received 7 October 2013; accepted 13 December 2013; published online 7 January 2014)

The charge injection from metallic electrodes into hole transporting layers of organic devices often suffers from deviations from vacuum-level alignment at the interface. Even for weakly interacting cases, Pauli repulsion causes an interface dipole between the metal and conjugated organic molecules (COMs) (so called “push-back” or “cushion” effect), which leads notoriously to an increase of the hole injection barrier. On the other hand, for chalcogenol self assembled monolayers (SAMs) on metal surfaces, chemisorption via the formation of chalcogen-metal bonds is commonly observed. In these cases, the energy-level alignment is governed by chalcogen-derived interface states in the vicinity of the metal Fermi-level. In this work, we present X-ray and ultraviolet photoelectron spectroscopy data that demonstrate that the interfacial energy-level alignment mechanism found for chalcogenol SAMs also applies to seleno-functionalized COMs. This can be exploited to mitigate the push-back effect at metal contacts, notably also when COMs with low ionization energies are employed, permitting exceedingly low hole injection barriers, as shown here for the interfaces of tetraseleno-tetracene with Au(111), Ag(111), and Cu(111). © 2014 AIP Publishing LLC. [<http://dx.doi.org/10.1063/1.4858856>]

I. INTRODUCTION

A maximum understanding and control of the organic/metal (O/M) interface is of paramount importance for the realization of efficient devices with well-defined morphologies in the growing field of organic electronics. To facilitate efficient charge transfer at O/M interfaces, low hole injection barriers (HIB) are needed,^{1,2} which, when assuming vacuum-level alignment, are related to a small ionization energy (IE) of the organic material and/or a high work function (ϕ) of the metal. However, when molecules are brought into contact with clean metals, the initial metal ϕ is usually altered due to the formation of an interface dipole, which can originate from a variety of effects.³ In the case of noble metals and physisorbed molecules without permanent dipole moment, one major contribution has been identified: The electron density spilling out into vacuum at the clean metal surface is “pushed back” by the molecules due to Pauli repulsion.^{1,4} In this case the initial metal work function is reduced and thus the HIB is significantly larger than expected from simple vacuum-level alignment. The magnitude of the push-back effect is mainly controlled by the adsorption distance of the conjugated organic molecule (COM) and does not involve a chemical hybridization of its frontier molecular orbitals and the metal states.⁵⁻⁷ For chemisorbed molecules, in contrast, a chemical molecule-metal interaction can further

change the charge rearrangement between molecule and surface. The resulting interface dipole can be of both signs, and competing effects can also cancel each other and thus mimic vacuum-level alignment. For instance, molecular acceptors with typically large electron affinities (EAs) (and consequently also large IEs) were found to form a charge transfer complex with the metal and thus to counterbalance the push back effect⁸⁻¹⁰ and, when employed as interlayers, to thereby decrease the HIBs between metals and active overlayers.^{9,10} However, the acceptor molecules have often a low molecular weight and are thus prone to interlayer diffusion,¹¹⁻¹³ which hinders controlled device fabrication. Thus, the combination of (i) a low IE and (ii) the capability to mitigate the push-back effect at the metal electrodes in one COM is clearly desirable, since it would eliminate the necessity for an additional interlayer. Conveniently, the charge rearrangement at the O/M interface depends also on the COM chemical structure and, for example, the bonding of specific substituents to the metal surface.¹⁴ Clearly, in order to combine the two dissimilar attributes (i) and (ii), which in the interlayer architecture are carried by donor and acceptor molecules, respectively, the semiconducting properties of the COM and its chemical bond to the metal must be electronically largely independent. This was indeed observed for selenolate- and thiolate-self-assembled monolayers (SAMs) on several coinage metal surfaces,^{15,16,86} for which the adsorption-induced charge

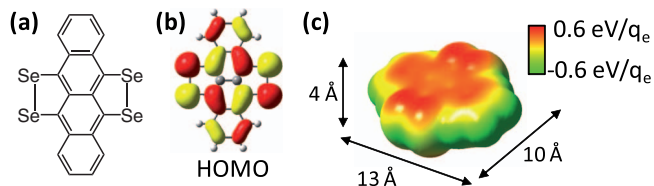


FIG. 1. (a) Chemical structure, (b) HOMO isodensity plot (iso value: $0.13 \text{ e}/\text{\AA}^3$), and (c) electrostatic potential map and geometric dimensions of tetraseleno-tetracene (TSeT).

rearrangement does not invoke the orbitals of the SAM core, and the energy-level alignment at the O/M interface is governed by an alignment of the chalcogen-derived states to the metal Fermi-level.^{17–20}

To test how chalcogeno-functionalization of COMs affects their energy level alignment with metal contacts, we selected tetraseleno-tetracene (TSeT, chemical structure in Fig. 1), which can be seen as derived from tetracene by substitution of four hydrogen atoms by selenium atoms (which is predicted to be a better electronic coupling group than sulfur^{21,22}). It was first synthesized more than 50 years ago²³ and mostly studied due to its ability to form radical-cation salts, which were found to be highly conducting.^{24,25} In these salts TSeT acts as donor, and it was shown by electrochemical measurements and calculations that the IE of tetracene decreases significantly by the selenium substitution (even below that of pentacene).²⁶ With our photoemission results on vacuum-deposited TSeT thin films on the (111)-surfaces of coinage metals we demonstrate that it is indeed possible to combine the special energy-level alignment situation of SAMs with the organic semiconductor properties of TSeT, resulting in extremely small HIBs.

While small HIBs at O/M interfaces are an energetic prerequisite for many devices, layer-by-layer growth of the organic material is often desired in addition (e.g., in organic light-emitting diodes, OLEDs), which is also essential for a clear assessment of the energy-level alignment at the immediate TSeT/metal interface. However, our photoemission experiments show that TSeT exhibits pronounced 3D island growth when deposited onto substrates kept at room temperature (RT). By cooling the metals to 77 K (LT) during TSeT deposition, island formation is kinetically hindered, resulting in kinetically limited layering of lying-down molecules. For a controlled assessment of how the interplay of substrate-molecule and intermolecular forces affects the film morphology,^{27–31} annealing procedures of LT-grown TSeT films were performed.

II. EXPERIMENTAL DETAILS

Au(111), Ag(111), and Cu(111) single crystals were cleaned by repeated heating and Ar-ion sputter cycles. A (100) oriented p-doped silicon single crystal (Siebert Consulting, prime grade) with a native oxide layer (SiO_x) was used without further treatment. TSeT was purchased from Ambinter (France) and purified by recrystallization in trichlorobenzene. TSeT films were vacuum deposited from resistively heated quartz crucibles for all experiments.

RT X-ray and ultraviolet photoelectron spectroscopy (XPS/UPS) experiments were performed at the end station SurICat (beamline PM4)³² at the synchrotron light source BESSY II (Berlin, Germany). TSeT films were grown in the preparation chamber (base pressure $<1 \times 10^{-8}$ mbar) and transferred to the analysis chamber (base pressure 2×10^{-10} mbar) without breaking ultrahigh vacuum (UHV) conditions. XPS (UPS) was performed using a photon energy of 620 eV (35 eV). Photoemission spectra were collected with a hemispherical electron energy analyzer (Scienta SES 100, 120 meV energy resolution) with angles between sample and incident beam of 60° and 15° for electron emission angles of 0° and 45° , respectively. The film thickness was monitored with a quartz crystal microbalance. The secondary electron cutoff (SECO) was measured with -10 V bias applied to the sample.

LT and annealing experiments were done at Chiba University. Film growth and characterization were done in the same UHV chamber (base pressure 4×10^{-10} mbar). TSeT was evaporated onto substrates kept at 77 K. A cooling shield ($T = 30$ K) surrounding most of the sample holder largely reduced sample surface contamination due to adsorption of residual gas. Since this chamber was not equipped with a thickness monitor, the rate for the evaporation source was calibrated beforehand in another UHV chamber with a quartz crystal microbalance and set to ca. $2 \text{ \AA}/\text{min}$ (which might have slightly decreased with time). UPS experiments were performed with a HeI UV light source and a hemispherical electron energy analyzer (Scienta R3000). The angle between the incident beam and the sample was fixed to 65° for electron emission angles of 0° and 45° ; details of the measurement geometry can be found in Ref. 33. The sample was biased with -3 V for SECO measurements. The energy resolution was 80 meV at RT. Note that relative differences of the energetic positions of SECO and peak maximum/onset within one set of experiments can be determined with a smaller uncertainty.

Density functional theory (DFT) calculations for a free TSeT molecule were performed with Gaussian09 (Revision A.02)³⁴ using the PBE0 hybrid exchange-correlation functional³⁵ and a 6-31G** contracted-Gaussian basis set.^{36,37}

III. RESULTS AND DISCUSSION

A. Room temperature film growth (interface region)

To establish whether TSeT indeed interacts with the metals Au and Ag via its seleno side groups we first performed XPS experiments that should yield characteristic core level binding energy shifts upon specific strong interactions. A film of nominal 100 \AA TSeT deposited on SiO_x , for which no significant interaction is expected at the interface, served as reference system for bulk-like spectral features. The $\text{C}1s$ and $\text{Se}3d$ spectra are shown in Fig. 2(a). For the $\text{C}1s$ spectrum, the contribution of the residual carbon contamination of the SiO_x substrate is subtracted. The remaining spectrum (residue) can be fitted with one Voigt peak at 284.75 eV. The $\text{Se}3d$ region contains two doublets of very different intensity. The binding energy (BE) of the main feature ($\text{Se}3d_{5/2}$ at 55.9 eV)

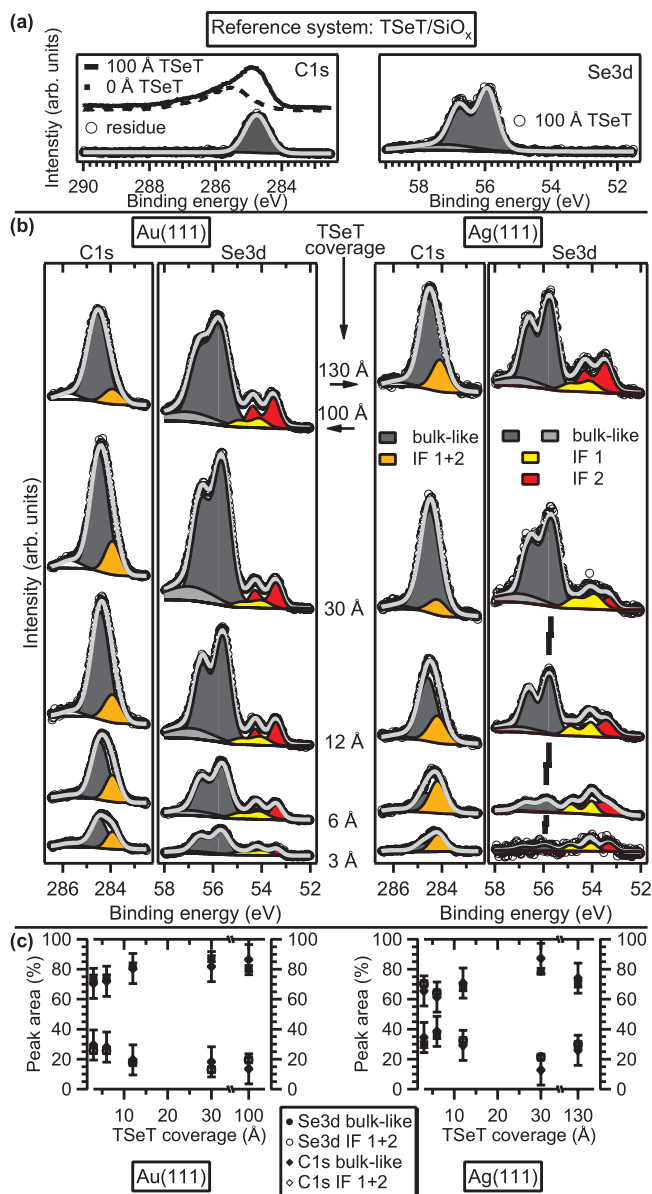


FIG. 2. Se3d and C1s core level spectra for (a) 100 Å TSeT/SiO_x; For the C1s spectrum, the contribution due to the carbon contamination of the SiO_x substrate (=0 Å TSeT) was subtracted as shown and (b) TSeT films of indicated coverage on Au(111) (left) and Ag(111) (right). For the Se3d spectra, the background due to the Au5p_{3/2}- and the Ag4p-contribution was subtracted, respectively (not shown). For both core levels, the spectral intensity which corresponds to the species found also for TSeT/SiO_x (shown by the black and grey filling) is termed “bulk-like.” For the Se3d signal, two additional contributions at lower binding energy, identified as interface species (IF 1 and IF 2, IF 1 has the larger binding energy of the two), can be resolved. For the C1s signal, only one additional peak at lower binding energy (containing both IF species) can be resolved by a fitting procedure as detailed in the text. (c) Fractions of bulk-like and IF species in the Se3d and C1s spectra [as found by the fits of the core levels in (b)] as function of TSeT coverage.

compares well to what was found for bulk TSeT.³⁸ The very weak and also broader feature at ca. 57 eV BE is most likely due to a shake-up process, as was observed for the closely related molecule tetrathio-tetracene (TTT).³⁸

In Fig. 2(b) the Se3d and C1s spectra for several coverages of TSeT on Au(111) (left) and Ag(111) (right) are shown. The Se3d region overlaps with the energy positions

of Au5p_{3/2} and Ag4p levels, and the presented spectra have been corrected for photoelectron intensity stemming from these substrate features by a simple subtraction procedure (not shown). Starting from nominal sub-monolayer TSeT coverage (ca. 3 Å), we observe four Se3d doublets for each of these two metals. The two features at higher BE agree with the two bulk-like peaks observed for TSeT/SiO_x (*vide supra*). The two features at lower BE (Se 3d_{5/2} at 54.0 eV and 53.5 eV) are not present in the reference spectra for films on SiO_x, thus they must be attributed to TSeT interacting with the metal surfaces and are therefore referred to as interface species (IF 1 and IF 2, respectively).

Like the Se3d spectra, also the C1s spectra of TSeT/Au(111) and TSeT/Ag(111) differ from these of the TSeT film on SiO_x, as can be clearly seen by the peak asymmetry, particularly for low coverages. In a simple fit model, we attribute one contribution in the C1s spectra to the bulk-like species, and by fixing the energy difference between Se3d_{5/2} and C1s to 228.8 eV (as found for “bulk” TSeT on SiO_x) we find the second C1s contribution at 0.5 eV lower BE (i.e., a too large energy difference to be only due to a difference in photo-hole screening efficiency), which we thus assign to the interface species. This assumption is supported by the good agreement of the relative spectral weights of bulk-like and interface (IF 1 + IF 2) contributions for both elements’ core levels, as illustrated as a function of coverage in Fig. 2(c). Note that the C1s to Se3d peak area ratio is consistent with the chemical formula of TSeT for all coverages. Some spectral intensity is also observed at ca 285.5 eV, which was not seen for TSeT/SiO_x [Fig. 2(a)]. This feature, which is too small to notably contribute to the quantitative analysis, probably stems from those carbon atoms of TSeT that are bound to selenium atoms, and, thus, undergo a different chemical shift upon chemisorption compared to the other carbon atoms.¹⁴ Notably, the BE values of the interface species for Se3d and C1s are very similar to those found for selenolate SAMs on Au(111) and Ag(111), where the selenium atoms are covalently bound to the metal.^{39–41} This strongly hints towards a similar interaction in terms of strength and bond mediation (i.e., via the selenium atoms) also between TSeT and Au and Ag.

In the chalcogenolate SAM-related literature, different explanations can be found for the occurrence of *two* Se3d-peaks with BEs similar to IF 1 and IF 2 found for TSeT/Au(111) and TSeT/Ag(111) [Fig. 2(b)]: For selenolate and thiolate SAMs on Ag(111) and Au(111), BE differences of the chalcogen core levels between films of different SAM types^{42,43} and also within the same film⁴⁰ comparable to the 0.5 eV difference between IF 1 and IF 2 have been observed and were explained with *differently bound chalcogenolate species*. In particular, a systematic variation with the number of methylene groups was found for oligophenyl-substituted alkanethiolate SAMs (so-called odd-even effects)^{42,43} and explained with differently strained sulfur-metal bonds.⁴⁴ On the other hand, for benzeneselenol/Au(111)³⁹ and biphenyl methylenethiol/Ag(111),⁴³ two core level peaks have been attributed to two *chemically different chalcogen species on the surface: chalcogen atoms in chalcogenolate molecules* [at higher BE, which would correspond to IF 1 in Fig. 1(b)] and

chalcogen atoms abstracted from the molecules [at lower BE, which would correspond to IF 2 in Fig. 2(b)]. In the present case, given the chemical structure of TSeT [Fig. 1(a)], containing four selenium atoms that are not spaced in registry with the Ag(111) or Au(111) lattice, it is conceivable that the selenium atoms of TSeT form differently strained bonds with the Au and Ag surface. In addition, while we find TSeT to lie mostly flat on Au(111) and Ag(111) from the LT experiments (*vide infra*), it is possible that some TSeT molecules adopt an inclined (and thus differently bound) adsorption geometry, which was indeed observed for TTT/Au(111) from scanning tunneling microscopy (STM).^{45,46} These considerations allow rationalizing the observation of two interface species without invoking a breakage of Se–C bonds. However, with the insufficient atomistic-geometrical information for this particular system, we refrain from any further speculation.⁴⁷

Having established that TSeT molecules bind to the metal surfaces strongly via their seleno groups, we now examine how this affects the energy level alignment. Fig. 3 shows UPS spectra for some of the same samples already discussed with XPS from Fig. 2(b), i.e., in the TSeT monolayer range. Thicker TSeT films will be discussed after LT and annealing sections (Secs. III B and III C, respectively), in order to allow a comprehensive discussion once both RT and LT data

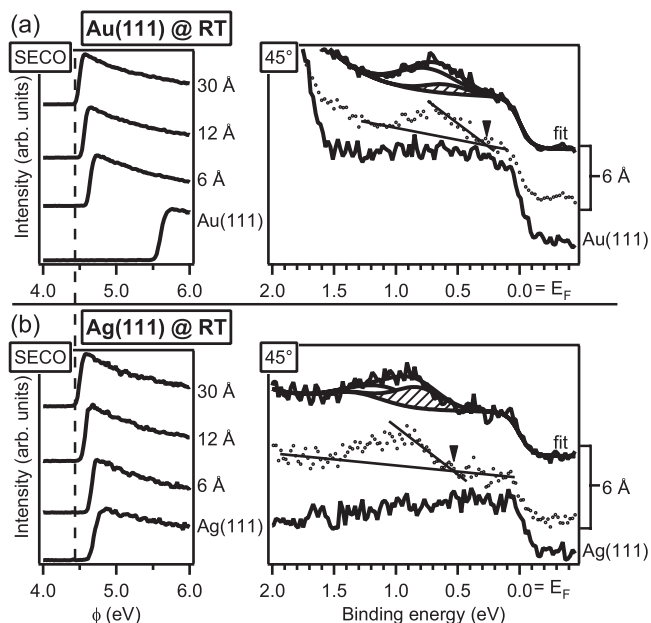


FIG. 3. Room temperature UPS results of (a) Au(111) and (b) Ag(111) for the pristine metals and after deposition of the indicated nominal TSeT coverages. On the left, the SECO region is shown for TSeT coverages up to the approximate saturation of the vacuum level shift (30 Å). A dashed line illustrates the common $\phi = 4.45$ eV at 30 Å in both cases. In the right figure part, the valence band region close to E_F is shown (measured with an angle of 45° between sample normal and detector). For both (a) and (b), only the spectrum for a TSeT film close to the nominal monolayer coverage (6 Å) is presented, which is used to determine the HOMO energetic position by a simple onset procedure, as illustrated for the dotted spectra. In addition, a fit in agreement with the findings from the LT data (*vide infra*) is presented for the identical spectra shown as continuous lines. The peak filled with dashed lines corresponds to the two interface species, and the one without filling accounts for the multilayer species. The relative intensities for the two fit contributions are approximated by the respective relative intensities determined from the core level fits presented in Fig. 2.

have been introduced. In the left part of Fig. 3 the SECO region is presented, which is used to determine the sample work function ϕ . Results for Au(111) and Ag(111) are reported in (a) and (b), respectively. The bottommost trace in each graph shows the spectra for the respective pristine metal surfaces. Up to 30 Å TSeT coverage, the work function of Au(111) is reduced by 1.05 eV (from an initial value of 5.50 eV) and by 0.15 eV on Ag(111) (from 4.60 eV). Thus, ϕ of 30 Å TSeT on both metals is 4.45 eV and the initial ϕ difference between Ag(111) and Au(111) of 0.9 eV is eliminated by deposition of the TSeT monolayer and the concomitant formation of an interface dipole ($\Delta\phi$). From the very different $\Delta\phi$'s we can conclude on markedly different charge density rearrangements upon TSeT/metal interface formation in the two cases. Interestingly, a fully analogous behavior was observed for thiolate SAMs on the same metals.⁴⁸ For these interfaces, theoretical modeling indicated that the adsorption-induced work function change is dominated by the charge transfer between the sulfur atom and the metal, which is driven by the initial metal ϕ , thus resulting in very similar ϕ values after SAM formation.^{17–20} The calculations found the same behavior for selenol and thiol docking groups. Therefore, the behavior of TSeT, i.e., yielding the same ϕ for TSeT/Au(111) and TSeT/Ag(111), together with the core level BEs that match those of selenolate SAMs, suggests that the selenium-metal bonds in these systems behave very similar to what was found for the SAMs. We therefore propose that the same energy-level alignment mechanism as found for the SAM/metal interface,¹⁸ also governs the energy level alignment at the TSeT/metal interface.

Note that $\Delta\phi$ for TSeT deposited on Au(111) is comparable to that induced by many *physisorbed* molecules, such as the prototypical organic semiconductor pentacene,^{49,50} which also compares well to TSeT in terms of IE and molecular structure,^{51,87,88} or, e.g., benzene.⁴ However, the $\Delta\phi$ induced by pentacene is due to the push-back effect, whereas XPS clearly showed chemisorption of TSeT on Au(111). The impact of the selenium substitution is even more pronounced for TSeT/Ag(111), where $\Delta\phi$ is significantly smaller than reported for physisorbed molecules like pentacene^{52,53} and other common COMs.^{10,54,55} Accordingly for TSeT, the push-back effect is to a significant extent counterbalanced by the charge density rearrangement induced by the seleno-Ag bond.

The low BE valence band region at an emission angle (θ) of $\theta = 45^\circ$ is presented in the right part of Fig. 3. For a nominal TSeT coverage of 6 Å on both Au(111) and Ag(111) we find a peak in the low BE valence region (Fig. 3) close to the Fermi-level (E_F), which was not observed for the pristine metals, and can be readily ascribed to emission from the orbital of chemisorbed TSeT which is derived from the highest occupied molecular orbital (HOMO) of free TSeT. The low BE onsets of emission determined with the simple procedure illustrated in Fig. 3 are at 0.25 eV and 0.5 eV for Au(111) and Ag(111), respectively.

From the evolution of ϕ as function of nominal coverage we conclude that the monolayer is closed only beyond 12 Å or 30 Å on both substrates, which is well beyond the nominal monolayer-equivalent coverage (4 Å). Therefore, 3D-island formation is preferred over metal surface wetting for TSeT

films deposited at RT. Accordingly, already films of very low nominal coverage not only contain TSeT molecules that are in contact with the metal surface, but also some that are located in multilayers, as is also supported by the XPS data in Fig. 2. In general, the ionization energies measured by UPS of molecules in the bulk and in contact with a metal surface are not the same, e.g., because the photohole screening efficiency of a metal is significantly larger than that of an all-molecular surrounding.^{56–58} Indeed, as we will show below for TSeT films grown at LT, the energy levels of multilayer TSeT molecules are at higher BE than the ones in contact with the metals. To account for this finding, which we will discuss in detail in Sec. III B, Fig. 3 also presents fits that account for both species, with the relative spectral intensities as found for IF and bulk-like species in XPS. Note that the less intense interface contribution of the HOMO-derived peak for TSeT/Au(111), as compared to TSeT/Ag(111) [Figs. 3(a) and 3(b), respectively], is consistent with the fact that multilayer molecules, which attenuate the interface signal, are much more abundant in the case of Au(111) [cf. Fig. 2(b)]. However, given the complex film morphologies, a detailed analysis of the HOMO-derived peaks is beyond the scope of the simple model employed.

B. Low temperature film growth

To clearly disentangle the energy levels right at the interface and in multilayers, which is to some extent impeded by the island growth mode at RT, TSeT films were also grown on Au(111), Ag(111), and Cu(111) single crystals cooled to 77 K (LT), whereby the tendency of TSeT to form islands was kinetically suppressed. Cu was added in this part of the study to extend the metal substrates towards typically higher reactivity with conjugated molecules. UPS spectra of the pristine metals at RT and LT, and for TSeT deposited on them at LT are reported in Figs. 4(a)–4(c), for Au(111), Ag(111), and Cu(111), respectively. When cooling Au(111) from RT to LT, ϕ decreases slightly from 5.43 eV to 5.27 eV and the surface state, visible at an emission angle $\theta = 0^\circ$, shifts to higher BE due to lattice contraction,⁵⁹ but does not decrease in intensity; thus Au(111) surface contamination due to adsorbates⁸⁹ is not impeding our results.⁶⁰ Analogous observations were made for Ag(111), where the ϕ decrease upon cooling to 77 K is only 0.02 eV, the surface state shifts to higher BE, and it increases in intensity as was reported before.⁵⁹ For Cu(111), the ϕ decrease upon cooling to 77 K is 0.3 eV. Furthermore, the surface state is almost completely quenched when reaching 77 K. We speculate that, despite our best efforts, the Cu(111) surface did suffer from notable residual gas molecule adsorption during the cooling process; consequently, the Cu results will be considered as preliminary.

1. Au(111)

Depositing ca. 2 Å TSeT gives rise to a peak in the valence electron region with its maximum at 0.6 eV BE, shown in the very right part of Fig. 4(a), which we assigned to emission from the HOMO of TSeT. This peak is clearly visible at a take-off angle of $\theta = 45^\circ$, while it is much less intense

for $\theta = 0^\circ$. Such a θ -dependence of the HOMO-related spectral intensity is due to the selection rules of the photoelectric process and can be attributed to flat-lying molecules for the HOMO symmetry of TSeT [a_u in the D_{2h} symmetry group for an isolated molecule as shown in Fig. 1(b)],⁶¹ consistent with the prevailing geometry also observed for TTT/Au(111) by STM.^{45,46} The maximum of the HOMO-derived peak for the 6 Å coverage is located at higher BE than for 2 Å, due to a second contribution with its maximum at 0.9 eV, as shown by the best fit in the $\theta = 45^\circ$ spectrum. The emergence of this feature in the valence spectrum is a good indication that at least a second molecular layer is present at this coverage. In view of the molecular dimensions shown in Fig. 1(c), this corroborates the reasoning that the first TSeT layer adsorbs flat-lying. The higher BE of the second layer can be explained by the less efficient photo-hole screening in multilayers compared to the monolayer in direct contact with the metal substrate.^{56–58} In addition, the TSeT molecules chemisorb on Au(111), and thus as the monolayer is chemically different from the multilayer TSeT molecules, which will result in different orbital energies.¹⁴

At this coverage of 6 Å ϕ has reached its minimum of $\phi_{ML} = 4.49$ eV. Together with the HOMO low BE onset at 0.2 eV we retrieve the IE of the TSeT monolayer on Au of $IE_{ML} = 4.7$ eV. No ϕ change occurs between 6 Å and 20 Å coverage, as expected for multilayer formation once the chemisorbed monolayer is completed. However, when going from 20 Å to 120 Å coverage, we find a small ϕ increase of 40 meV to 4.53 eV and a shift of the maximum of the HOMO-derived peak by the same amount towards E_F , i.e., a rigid shift. In Fig. 5, the HOMO maximum positions and ϕ values are summarized for all investigated coverages.

Such gradual energy level shifts when going from chemisorbed monolayer to multilayer are to be expected on general grounds, and have been reported frequently (e.g., Refs. 62 and 63), also for chalcogenolate SAM interlayers.⁶⁴ In the present case, the observed rigid parallel shift of HOMO and ϕ points to an electrostatic effect. We exclude a long range charge transfer caused by Fermi-level pinning of the lowest unoccupied molecular orbital (LUMO)^{65–68} or impurities^{52,69–71,90} (as required for the observed shifts to lower BE), since we would rather expect Fermi-level pinning to happen for the HOMO in view of its proximity to E_F (see also discussion below). The small shift might stem from polarization at the organic homo-junction, consisting of bulk-like TSeT on top of chemisorbed TSeT, similar to what was found in a recent theoretical study.⁷²

The peak full-width-at-half-maximum (FWHM) of the HOMO-derived peak of the 120 Å thick film is 0.5 eV, i.e., slightly larger than the 0.4 eV for the first and second layer, which indicates that the arrangement of molecules in the multilayer probably deviates from the flat-lying arrangement found for low coverages.

The continued TSeT deposition up to a total coverage of ca. 250 Å, which corresponds to several tens of monolayers, led to a rigid shift of the valence spectrum of ca. 0.1 eV to higher BE and a ϕ shift of 0.13 eV (leaving $IE_{thick} = 4.9$ eV essentially constant), together with a broadening of all peaks in the valence band. These observations are

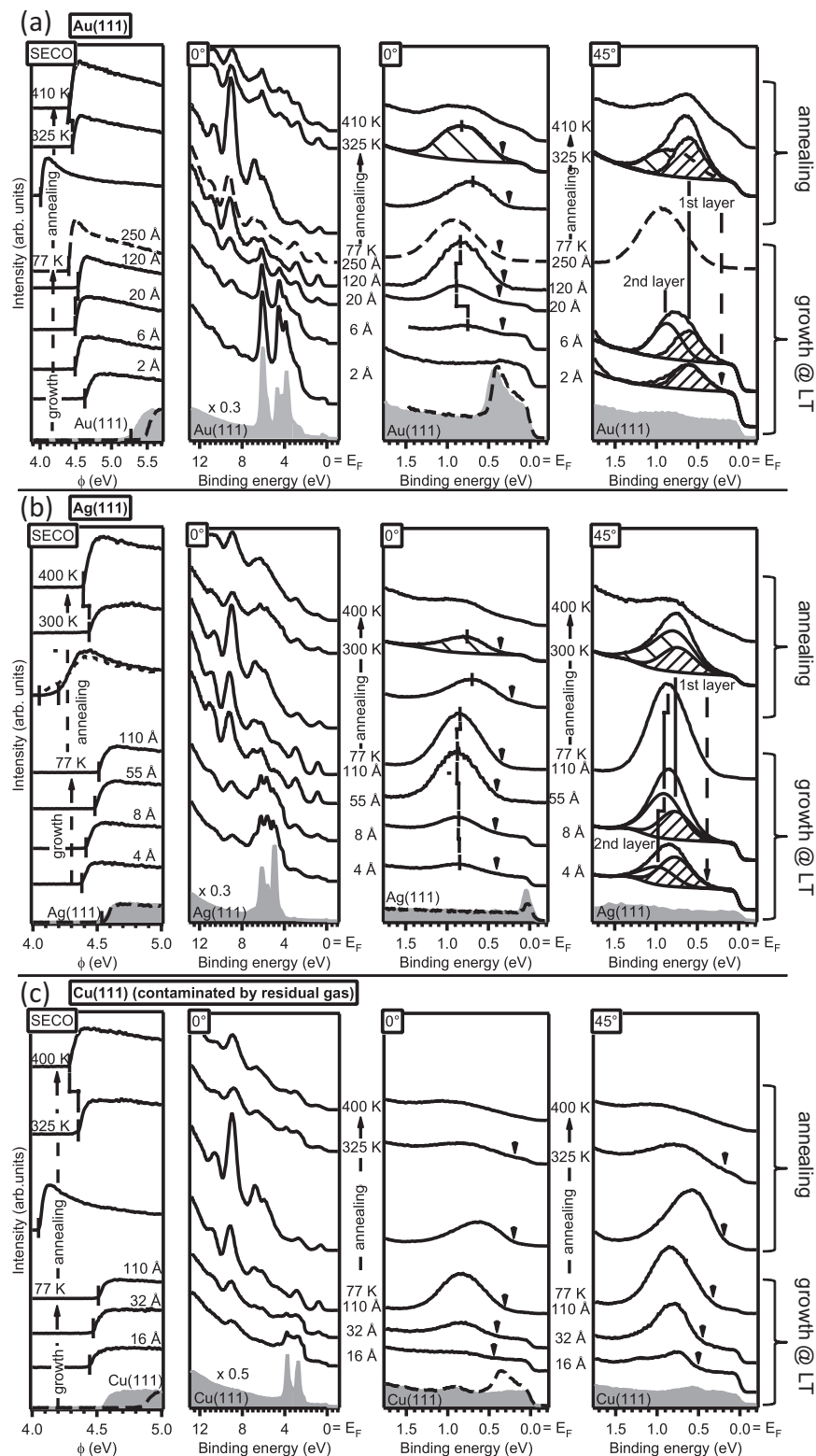


FIG. 4. UPS results for TSeT films grown on (a) Au(111), (b) Ag(111), and (c) Cu(111) with the samples held at 77 K and during subsequent annealing to 400 K. Shown are, from left to right, the SECO region, the valence band region at electron emission angle $\theta = 0^\circ$, and zooms into the region close to E_F at $\theta = 0^\circ$ and $\theta = 45^\circ$. For (a)–(c), in each case the following samples are presented. Bottom: The pristine metals before (dashed lines) and after decreasing the sample temperature to 77 K (solid grey). Middle (labeled “growth”): TSeT films of the indicated nominal coverage deposited at 77 K. For (a) and (b), the first layer (filled with slanted lines with positive slope) and second layer contribution (without filling) for the lowest two TSeT coverages are also shown. The dashed spectra in (a) show indications of sample charging as detailed in the main text. Top (labeled “annealing”): TSeT films of the respective maximum thickness during subsequent heating to the indicated sample temperature, or in the indicated sample temperature range. For (b) and the annealing temperature between 77 K and 300 K, two SECO spectra measured at slightly different sample spots are shown, which both show signs of multilayer dewetting. The determination of a clear SECO spectrum as in (a) and (b) was not possible for this system and the SECO onset at lowest kinetic energy will be used for further analysis, since it gives the best guess for the situation which is still governed by ϕ of multilayer molecules. For (a) [(b)] and 325 K [300 K], the contributions used for the subtraction procedure described in the main text are shown with a filling of slanted lines with negative slope.

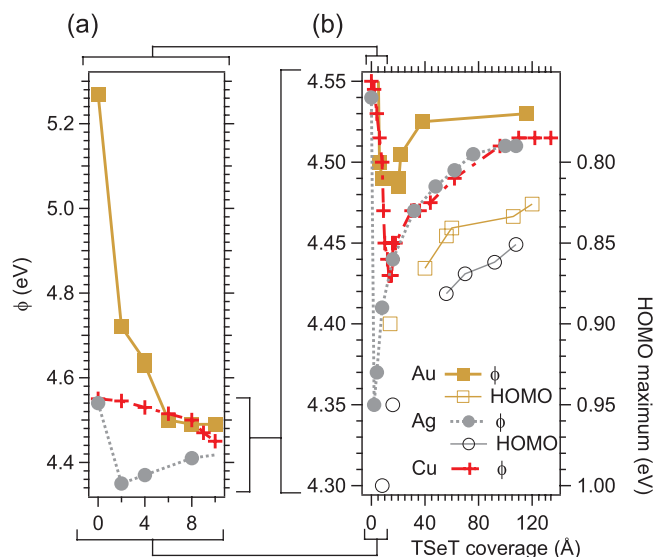


FIG. 5. (a) Evolution of ϕ as function of TSeT coverage (up to ca. 2–3 nominal monolayers) and with different substrates [Au(111), Ag(111), and Cu(111)] (samples were cooled to 77 K). (b) The same as (a) but including also thicker films. Note that the energy axis was decreased to emphasize the small ϕ increase with increasing coverage. The maximum of the HOMO-derived peak (HOMO maximum) is shown for Au(111) and Ag(111) to illustrate the parallel energetic shift of HOMO maximum and ϕ . For multilayer films, the values are plotted as symbols with connecting lines. For lower film thicknesses, interface effects predominate and the HOMO maxima were derived indirectly, as shown in Figs. 4 and 5. These values are plotted without the connecting lines. The ϕ values for Cu(111) are reported to illustrate their consistency with the other systems, despite the initial slight contamination of the Cu(111) surface by residual gas molecules and the qualitative differences of this system discussed in the main text.

probably related to positive charging of the molecular film during photoemission.^{73,74}

2. Ag(111)

The SECOs for selected TSeT coverages on Ag(111) are shown in the left part of Fig. 4(b). The ϕ evolution derived from these and further coverages, plotted in Fig. 5, are now discussed first, which allows for a discussion of subtle changes in the energetic position of the HOMO-derived peak later on. We first observe a sharp ϕ decrease to a minimum of $\phi_{\text{ML}} = 4.35$ eV at 2 Å, which corresponds to a change of -0.19 eV when compared to pristine Ag(111). We observe no further decrease when going beyond this coverage. Instead, already at 4 Å we find that ϕ increases slightly by 20 meV, which marks the start of a gradual increase of in total 0.16 eV for the final coverage of 110 Å. Note that this behavior is qualitatively the same as was found for Au(111), and the ϕ value at ca. 110 Å, $\phi_{\text{thick}} = 4.51$ eV, for TSeT/Ag(111) differs by only 20 meV from ϕ_{thick} for TSeT/Au(111). Notably, as can be seen in Fig. 5, we thus find different values for the ϕ shift at the [bulk-like TSeT]/[chemisorbed TSeT] homo-junction in the cases of Au(111) and Ag(111), which results in identical energy level alignments for the multilayer films with respect to the metal Fermi level.

With the coverage-dependent ϕ evolution at hand, we now turn to the valence region. For 4 Å TSeT/Ag(111), the HOMO-derived peak varies in intensity when comparing

$\theta = 0^\circ$ and 45° in a very similar way as we found for 6 Å TSeT/Au(111). Therefore, we conclude on a similar adsorption geometry of the monolayer, i.e., flat-lying. This is further supported by the fact that the minimum of ϕ is found between 2 Å and 4 Å coverage, which agrees well with the value that marked the onset of the formation of the second layer on Au(111). Since for a coverage of 6 Å TSeT on Au(111) we observed that the HOMO-derived feature contains a second contribution at higher BE, we conjecture that the same is also true for 4 Å TSeT/Ag(111). However, the assignment of two contributions at different BEs is less obvious in the latter case, as is apparent from almost identical peak maxima found for the HOMO-derived peak throughout the coverage range from 4 Å to 55 Å. Still, as indicated in Fig. 4(b) for $\theta = 0^\circ$, a small shift of about 10 meV when going from 4 Å to 8 Å and another of ca. 20 meV when going to 55 Å coverage indicate a change of BE between first layer and subsequent layers. A preliminary fitting (which is justified by our findings from annealing experiments) of the HOMO-derived peak for 4 Å and 8 Å coverage yields a second contribution to be located at 1 eV for 4 Å and 0.95 eV for 8 Å, which is exactly what we expect for the HOMO of multilayer molecules if we extrapolate the rigid shift of ϕ and HOMO, found for higher coverages in Fig. 5, to the low coverage regime. We therefore conclude that the HOMO of monolayer of TSeT on Ag(111) peaks at 0.8 eV and its onset is at 0.4 eV [shown in Fig. 4(b) for $\theta = 45^\circ$], which gives an only slightly higher $\text{IE}_{\text{ML}} = 4.75$ eV than was found for TSeT/Au(111) (cf. Fig. 6).

3. Cu(111)

The monolayer region of TSeT on Cu(111) is discussed in less detail than for the other two metals for the following reasons: First, the specific experiments that were indicative for the monolayer region on Au(111) and Ag(111), namely, very thin coverages and a multilayer film annealed to ca. RT, give much broader features in the case of Cu(111) as can be seen in Fig. 4. This indicates that TSeT reacts qualitatively different with Cu(111) compared to the other two metals. A qualitative difference in bond formation has also been found for (solution-processed) benzeneselenol/Cu(111) when compared to Au(111) and Ag(111).^{75,76} In addition, as mentioned before, the Cu(111) surface was not completely clean due to adsorbed residual gas molecules at LT.

When going beyond the coverage regime for which the spectra contain significant intensity from the direct TSeT/Cu(111) interface, energy position and overall behavior of the HOMO-derived peak and ϕ agree with what was found for multilayer films on the two other metal substrates. The ϕ evolution is included in Fig. 5 and is identical with the one for Ag(111). The continuous HOMO shift to lower BE with increasing coverage can be seen from the onsets indicated in the right part of Fig. 4(c).

Thus, even if the information on the monolayer contains the mentioned uncertainties, the overall energy level alignment of TSeT/Cu(111) follows the same trend as observed for TSeT/Au(111) and TSeT/Ag(111) (Fig. 4). The ϕ

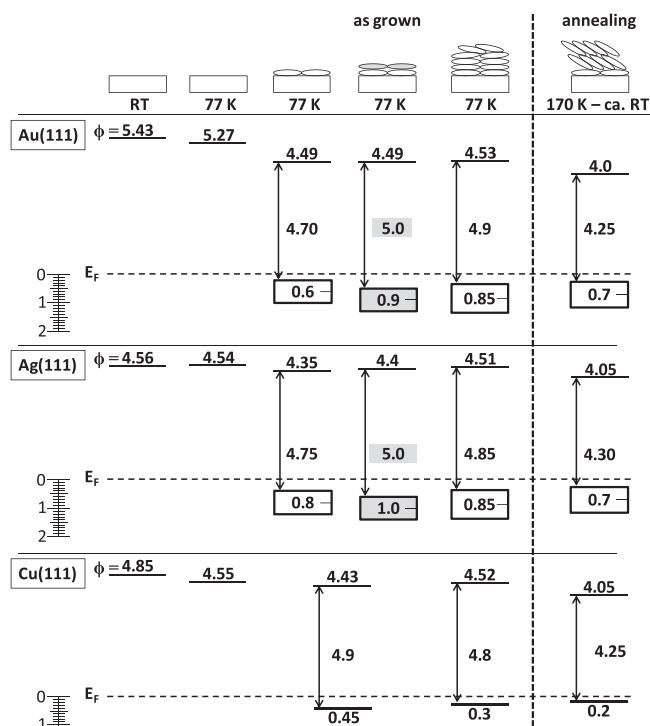


FIG. 6. Energy level diagrams (bottom) and morphology models (top) for the following systems. From left to the vertical dashed line: the pristine metals at room temperature (RT) and 77 K, the first TSeT layer, the second TSeT layer, and a multilayer TSeT film for a sample temperature of 77 K. Very right: The multilayer TSeT film during a subsequent annealing, beyond 170 K and just before room temperature (RT) is reached. The respective substrates and a scale bar for positive binding energies in eV are shown on the left. For Au(111) and Ag(111), the HOMO maxima are given and the peak widths are indicated by the rectangles ranging to the peak onsets. Only the onsets are shown for Cu(111) and first and second layer are not differentiated because of the qualitative differences of this system discussed in the main text. In all cases, the onsets are used for determining the presented ionization energies.

minimum in this case is in between the ϕ_{ML} values for the two other metals (Fig. 5). The present UPS results therefore indicate that the TSeT energy levels are similarly pinned on all three metal surfaces, consistent with what was observed for several thiol SAMs.⁴⁸

C. Annealing of films grown at low temperature

To be in a better position to discuss the film growth of TSeT at RT, we annealed the multilayer films deposited at LT by slowly increasing the sample temperature up to ca. 400 K over a time of ca. 15 h. The corresponding spectra are included in Fig. 4. The observations obtained are almost identical for all metals and will be discussed in detail for Au(111); only (small) differences observed for the other two metals will be discussed thereafter.

1. Au(111)

Starting with the sample at ca. 170 K, ϕ gradually decreases from 4.53 eV to 4.0 eV, while the HOMO onset shifts from 0.35 eV to 0.25 eV BE, i.e., the IE decreases by more than 0.6 eV. This temperature-induced process can be explained by gradual dewetting of TSeT from Au(111),

as also observed, e.g., for pentacene/Au.²⁸ This allows the molecules to rearrange (most likely a transformation from an amorphous to a polycrystalline film), which can impact IE for the following two reasons:

First, a better/closer molecular packing can increase the intermolecular screening, which was found to decrease the IE by up to 0.3 eV when going from disordered to crystalline films,^{77,78} and can explain part of the observed IE difference. Second, the orientation of the molecules with respect to the substrate can change,^{27,29,79} which was shown to significantly influence the IE.^{54,79,80} In the present case, a reorientation is indeed indicated by a change of the relative peak intensities in the valence region. The features higher in BE than ca. 5 eV are much more intense than before annealing started, while the peaks at lower BE decrease in intensity. The latter ones are derived from π -orbitals, while the former ones are mainly from σ -orbitals, as illustrated in more detail in Fig. 7. In accordance with similar systems,^{29,79} the observed intensity variation can therefore be interpreted as an increasing inclination of the backbone of the TSeT molecules (“lying-to-standing” transition). Such a transition is consistent with the observed IE decrease, since both, the Se and H

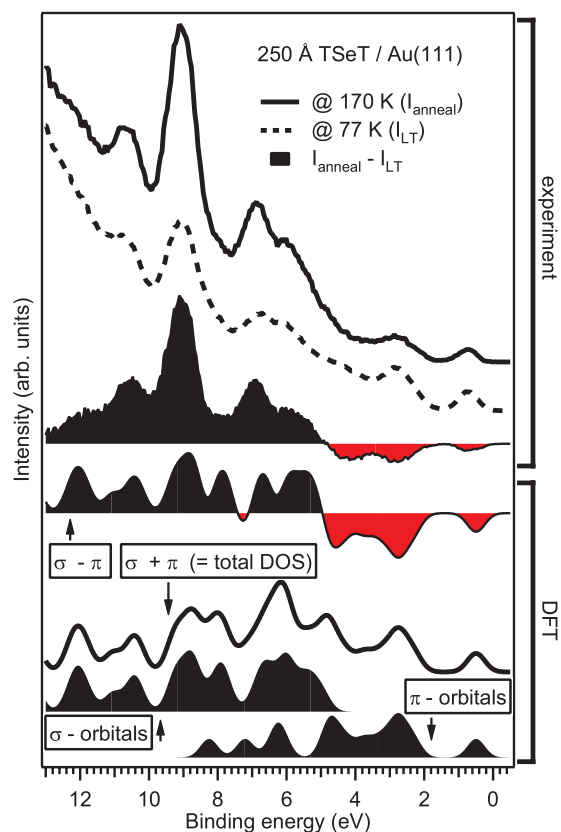


FIG. 7. Top part (labeled “experiment”): UPS spectra obtained before and during the annealing of a multilayer TSeT-film on Au(111) [the same as shown in Fig. 4(a)] and the difference spectrum illustrating where the annealing induces an intensity increase (black solid) and decrease [red (grey) solid]. Bottom part (labeled “DFT”): Calculated density of states (DOS), broadened by Gaussians with FWHM = 0.6 eV) belonging to π - and σ -orbitals (black solid, at bottom as labeled). Also shown are the total DOS (black line) and a difference spectrum indicating where σ -orbitals are more (black solid) and less important [red (grey) solid] for the DOS than the π -orbitals. Spectra have been shifted to align the HOMO maxima.

atoms have a positive partial charge,³⁸ while the π -electrons create a negative partial charge above and below the TSeT backbone. This results in a significantly anisotropic potential of an isolated TSeT molecule, as shown in Fig. 1(c), which translates to an IE decrease between a film of flat-lying and inclined molecules, which is further detailed in Refs. 80–82. Reorientation-induced IE decreases of comparable magnitude were reported before.^{54,79,80} Note that for lying-to-standing transitions of related molecules often a constant ϕ is observed and the change in IE is reflected only by a shift of the molecular levels.^{54,55} This is not the case for TSeT on Au. The HOMO level is very close to E_F already at LT, and the orientation-induced movement of the HOMO would bring it even above E_F , i.e., into extreme electronic non-equilibrium. In return, electrons are transferred from the TSeT HOMO to the metal, i.e., pinning sets in. Consequently, a significant dipole is built up as evidenced by the ϕ decrease. This ensures that also the reoriented molecules with lower film IE have their HOMO below E_F . The apparent finite energy difference between HOMO-onset and E_F can be rationalized by the tailing HOMO gap states, which are not accessible with the experimental sensitivity of our setup but should show up in specifically dedicated measurements.^{83,84}

When reaching ca. 325 K, ϕ increases again (gradually over ca. 1 h) to $\phi = 4.45$ eV, which is similar to ϕ_{ML} and ϕ_{thick} . Substrate features can now be seen again in the valence region, in particular the Au d-band, between 2 eV and 7 eV BE, and also the Fermi edge. Obviously, annealing leads to a dramatic change of the aspect ratio of the multilayer film, from quasi-2D to pronounced 3D. Therefore, the signal contribution from multilayer areas is reduced, i.e., the valence signal from the monolayer appears prominently and ϕ is increased due to the area-averaging of the SECO measurement. When comparing the HOMO-derived peak at $\theta = 0^\circ$ and $\theta = 45^\circ$ emission angle, additional intensity at lower BE can be seen for the latter case. The difference spectrum gives a peak that agrees very well in energy position and shape with the spectrum of the 2 Å film during the initial deposition sequence. This indicates that the monolayer does not dewet and reorient up to this temperature.

Increasing the sample temperature up to 380 K causes only a slight broadening of the valence features (not shown). However, at 400–410 K the intensity of the molecular features reduces drastically and irreversibly; when going back to RT the spectrum remains unchanged. This final annealing step also induces a ϕ decrease of 0.05 eV. The origin of these observations is likely desorption of intact molecules, probably accompanied by (substrate-mediated) chemical reactions and desorption of reaction products, similar to what was reported for benzeneselenolate/Au(111)^{39,85} and TTT/Au(111).⁴⁵

2. Ag(111)

On Ag(111) the dewetting (indicated by the beginning of the SECO shift to higher kinetic energies) sets in already at ca. 285 K [was ca. 325 K for Au(111)]. This difference between the two substrates agrees with the observation of more pronounced dewetting on Ag(111) observed during the RT

measurements (see below). However, another reason for the observation of dewetting already at lower temperatures might be the lower film thickness that we employed [less than half of that for Au(111)].

In addition, on Ag(111) the HOMO-derived peak of the film after dewetting (between 300 K and 380 K) has a different shape and its intensity varies differently as a function of θ than was observed for Au(111). Still, like for Au(111), a feature that is significantly higher in intensity at $\theta = 45^\circ$ than at $\theta = 0^\circ$ can clearly be seen. We therefore performed the same subtraction procedure as was performed in the case of Au(111) and found a feature with its maximum at 0.8 eV, which we attribute to the TSeT monolayer, consistent with the discussion for the LT-film growth above.

3. Cu(111)

On Cu(111), the shift of the SECO to higher kinetic energies sets in at around 300 K. As mentioned before, the HOMO-derived feature for the annealed film is very broad already at 325 K. However, another change in spectral shape and ϕ decrease is seen when the sample temperature reaches 400 K, showing that also in this case the TSeT film undergoes a significant structural change at this temperature.

D. Multilayer films grown at room temperature

With the conclusions drawn from the LT film growth and annealing experiments, we now turn back to RT-grown TSeT films and discuss the multilayer regime. Figs. 8(a) and 8(b) present the UPS data for TSeT films of the indicated nominal coverages grown on Au(111) and Ag(111), respectively. The respective XPS data were already presented in Fig. 2. The first observation is that even for the highest TSeT coverage on Au(111) (100 Å) as well as on Ag(111) (130 Å) [topmost spectra in Figs. 8(a) and 8(b), respectively], significant spectral intensity from the substrates – apparent from still visible Fermi edges and valence region shapes that are different for Au and Ag – can be observed. Since UPS is a very surface sensitive technique, with a sampling depth of only a few Å, this supports the notion of pronounced 3D island growth on both metal substrates at RT, as was discussed above based on XPS data and the SECO evolution only.

As discussed in Sec. III B, the contribution of the HOMO-derived peak that can be attributed to the multilayer is at higher BE than that of the monolayer, as can be seen in the fits shown for a coverage of 6 Å and an emission angle of $\theta = 45^\circ$ in the very right part of Fig. 8. With increasing coverage, this feature gradually shifts by ca. 0.25 eV to lower BE for Ag(111) and a (smaller) shift is observed also for Au(111); analogous shifts are seen in the bulk-like core levels. These shifts are in part of the same nature as those observed in the LT measurements, i.e., of electrostatic origin, with a corresponding shift of the SECO to higher kinetic energy not being observable due to 3D-island growth. However, the HOMO maxima observed for RT-grown multilayer films [0.6 eV and 0.75 eV for 30 Å TSeT on Au(111) and Ag(111), respectively] are at lower BE than observed for multilayer films

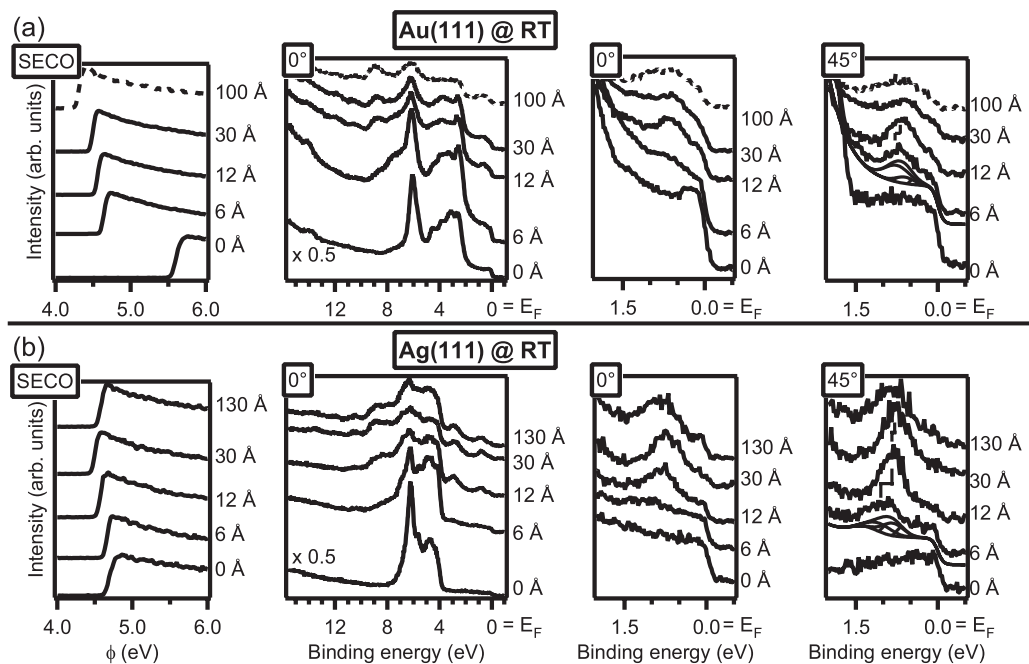


FIG. 8. Room temperature UPS results of (a) Au(111) and (b) Ag(111) for the pristine metals and after deposition of the indicated nominal TSeT coverages. Shown are, from left to right, the SECO region, the valence band region at $\theta = 0^\circ$, and zooms into the region around the E_F for $\theta = 0^\circ$ and $\theta = 45^\circ$. The dashed spectra in (a) show indications of sample charging.

grown at LT (0.85 eV in both cases). Recalling the observations during the annealing of the LT-grown films, this probably results from an increased inclination of TSeT molecules, with a further contribution from better screening in the RT-grown films (i.e., improved intermolecular order).

As can be seen in Fig. 2(b) (most clearly for the Se3d spectra and coverages less than 30 Å), the spectral intensity of the bulk-like (=multilayer) contribution in the case of Ag(111) is lower than for Au(111) for identical nominal coverages. This can be due to a lower sticking coefficient and/or more pronounced dewetting of multilayer TSeT molecules in the former case, which (both) means that TSeT molecules have less affinity to TSeT-monolayer-covered Ag(111) than to TSeT-monolayer-covered Au(111). This difference, which is consistent with the observed dewetting behavior of multilayer TSeT during the annealing of LT-grown films, is reflected in the following different observations for higher nominal TSeT coverages on Ag(111) and Au(111):

For Ag(111), the substrate features become more prominent when going from 30 Å to 130 Å TSeT coverage due to significant dewetting.⁶² Consistently, for this coverage step also the interface species in XPS become more intense [Fig. 2(c)] and an increase in intensity is also observed for the Ag3d core level (not shown).

For Au(111), on the other hand, the substrate contribution in the valence region decreases when increasing the coverage to 100 Å, evidencing that dewetting is less pronounced in this case. At the same time, the SECO shifts to lower kinetic energy and all peaks significantly broaden. A pronounced broadening is also observed for the core level peaks in XPS, and the bulk-like feature shifts to higher BE, i.e., rigidly with the SECO. These observations (which, as mentioned before, likely stem from photoemission-induced sample charging)

match those for the LT measurements, where, however, they were made only for a TSeT coverage of ca. 250 Å. This indicates columns of at least the same height for the RT-grown 100 Å TSeT film on Au(111), which further supports the notion of pronounced 3D island growth also in this case.

IV. CONCLUSIONS

TSeT at the interface with Au(111) and Ag(111) was studied with XPS, from which we find chemisorption via the selenium atoms. UPS results obtained for TSeT deposited on these metals and Cu(111) reveal different molecule-induced work function changes, which give rise to an almost identical work function for TSeT monolayers on the three metals (within 0.15 eV), while the initial metal work function values vary by almost 1 eV. This situation can be explained by charge density rearrangements at the seleno-metal-bonds resulting from Fermi-level pinning predominantly at the selenium-related levels. A seleno- (or chalcogeno-) functionalizing therefore offers a good strategy to counterbalance the push-back effect at the organic/metal interface, which reduces the work function in the case of physisorption. This is particularly relevant for TSeT/Ag(111), since Ag(111) has the lowest ϕ of the three metals. In this case, we find almost vacuum level alignment, and the low IE of TSeT allows a very low hole injection barrier (only 0.4 eV).

TSeT grows in a kinetically limited layer-by-layer fashion on Au(111), Ag(111), and Cu(111) when the samples are cooled to 77 K during deposition. Molecules in multilayers change orientation from lying to vertically inclined upon annealing and pronounced dewetting occurs. Consistently, TSeT exhibits 3D-island growth when the metal substrates are at RT. Therefore, despite the favorable energy

level alignment for hole injection from a metal, TSeT itself is not suitable for device applications. However, similar seleno-functionalization should be applicable also to organic semiconductors that have more favorable morphology and film growth, and, therefore, offers a promising route to fabrication of air-stable organic material with yet minimized hole injection barriers at noble metal contacts.

ACKNOWLEDGMENTS

The authors thank Michael Pätzelt, Jutta Schwarz, and Joachim Leistner (Department of Chemistry, Humboldt-Universität zu Berlin, Germany) for help with the recrystallization of TSeT, Ingo Salzmänn and Paul Zybarth (Department of Physics, Humboldt-Universität zu Berlin, Germany) for help with UV/vis spectroscopy, and Alexander Gerlach for discussions. This work was financially supported by the DFG (SCHR700/14-1, SPP1355, and SFB951), the Helmholtz-Energie-Allianz "Hybrid-Photovoltaik," the Global-COE Program of MEXT (G03: Advanced School for Organic Electronics, Chiba University) and a joint JSPS-NSFC project (Grant No. 612111116).

- ¹A. Kahn, N. Koch, and W. Gao, *J. Polym. Sci., Part B: Polym. Phys.* **41**, 2529 (2003).
- ²N. Koch, *ChemPhysChem* **8**, 1438 (2007).
- ³H. Ishii, K. Sugiyama, E. Ito, and K. Seki, *Adv. Mater.* **11**, 605 (1999).
- ⁴G. Witte, S. Lukas, P. S. Bagus, and C. Wöll, *Appl. Phys. Lett.* **87**, 263502 (2005).
- ⁵P. C. Rusu, G. Giovannetti, C. Weijtens, R. Coehoorn, and G. Brocks, *J. Phys. Chem. C* **113**, 9974 (2009).
- ⁶K. Toyoda, I. Hamada, K. Lee, S. Yanagisawa, and Y. Morikawa, *J. Phys. Chem. C* **115**, 5767 (2011).
- ⁷K. Toyoda, I. Hamada, K. Lee, S. Yanagisawa, and Y. Morikawa, *J. Chem. Phys.* **132**, 134703 (2010).
- ⁸L. Romaner, G. Heimel, J.-L. Brédas, A. Gerlach, F. Schreiber, R. L. Johnson, J. Zegenhagen, S. Duhm, N. Koch, and E. Zojer, *Phys. Rev. Lett.* **99**, 256801 (2007).
- ⁹N. Koch, S. Duhm, J. P. Rabe, A. Vollmer, and R. L. Johnson, *Phys. Rev. Lett.* **95**, 237601 (2005).
- ¹⁰J. Niederhausen, P. Amsalem, J. Frisch, A. Wilke, A. Vollmer, R. Rieger, K. Müllen, J. P. Rabe, and N. Koch, *Phys. Rev. B* **84**, 165302 (2011).
- ¹¹W. Gao and A. Kahn, *Appl. Phys. Lett.* **79**, 4040 (2001).
- ¹²S. Duhm, I. Salzmänn, B. Bröker, H. Glowatzki, R. L. Johnson, and N. Koch, *Appl. Phys. Lett.* **95**, 093305 (2009).
- ¹³P. Amsalem, A. Wilke, J. Frisch, J. Niederhausen, A. Vollmer, R. Rieger, K. Müllen, J. P. Rabe, and N. Koch, *J. Appl. Phys.* **110**, 113709 (2011).
- ¹⁴G. Heimel, S. Duhm, I. Salzmänn, A. Gerlach, A. Strozecka, J. Niederhausen, C. Bürker, T. Hosokai, I. Fernandez-Torrente, G. Schulze, S. Winkler, A. Wilke, R. Schlesinger, J. Frisch, B. Bröker, A. Vollmer, B. Detlefs, J. Pflaum, S. Kera, K. J. Franke, N. Ueno, J. I. Pascual, F. Schreiber, and N. Koch, *Nat. Chem.* **5**, 187 (2013).
- ¹⁵F. Schreiber, *Prog. Surf. Sci.* **65**, 151 (2000).
- ¹⁶J. C. Love, L. A. Estroff, J. K. Kriebel, R. G. Nuzzo, and G. M. Whitesides, *Chem. Rev.* **105**, 1103 (2005).
- ¹⁷P. C. Rusu and G. Brocks, *Phys. Rev. B* **74**, 073414 (2006).
- ¹⁸G. Heimel, L. Romaner, E. Zojer, and J.-L. Brédas, *Nano Lett.* **7**, 932 (2007).
- ¹⁹G. Heimel, F. Rissner, and E. Zojer, *Adv. Mater.* **22**, 2494 (2010).
- ²⁰G. Heimel, L. Romaner, E. Zojer, and J.-L. Brédas, *Acc. Chem. Res.* **41**, 721 (2008).
- ²¹S. N. Yaliraki, M. Kemp, and M. A. Ratner, *J. Am. Chem. Soc.* **121**, 3428 (1999).
- ²²L. Patrono, S. Palacin, J. Charlier, F. Armand, J. P. Bourgoin, H. Tang, and S. Gauthier, *Phys. Rev. Lett.* **91**, 096802 (2003).
- ²³E. P. Goodings, D. A. Mitchard, and G. Owen, *J. Chem. Soc., Perkin Trans. 1*, 1310 (1972).
- ²⁴I. Y. Shevyakova, L. I. Buravov, L. Kushch, E. B. Yagubskii, S. S. Khasanov, L. V. Zorina, R. P. Shibaeva, N. V. Drichko, and I. Olejniczak, *Koord. Khim.* **28**, 487 (2002).
- ²⁵P. Delhaes, C. Coulon, S. Flandrois, B. Hilti, C. W. Mayer, G. Rihs, and J. Rivory, *J. Chem. Phys.* **73**, 1452 (1980).
- ²⁶L. Zhang, S. M. Fakhouri, F. Liu, J. C. Timmons, N. A. Ran, and A. L. Briseno, *J. Mater. Chem.* **21**, 1329 (2011).
- ²⁷S. Müllegger, I. Salzmänn, R. Resel, G. Hlawacek, C. Teichert, and A. Winkler, *J. Chem. Phys.* **121**, 2272 (2004).
- ²⁸D. Käfer, C. Wöll, and G. Witte, *Appl. Phys. A* **95**, 273 (2009).
- ²⁹B. Winter, S. Berkebile, J. Ivanco, G. Koller, F. P. Netzer, and M. G. Ramsey, *Appl. Phys. Lett.* **88**, 253111 (2006).
- ³⁰B. Krause, F. Schreiber, H. Dosch, A. Pimpinelli, and O. H. Seeck, *Europhys. Lett.* **65**, 372 (2004).
- ³¹B. Krause, A. C. Dürr, F. Schreiber, H. Dosch, and O. H. Seeck, *J. Chem. Phys.* **119**, 3429 (2003).
- ³²A. Vollmer, O. D. Jurchescu, I. Arfaoui, I. Salzmänn, T. T. M. Palstra, Rudolf, J. Niemax, J. Pflaum, J. P. Rabe, and N. Koch, *Eur. Phys. J. E* **17**, 339 (2005).
- ³³S. Duhm, Q. Xin, S. Hosoumi, H. Fukagawa, K. Sato, N. Ueno, and S. Kera, *Adv. Mater.* **24**, 901 (2012).
- ³⁴M. J. Frisch, G. W. Trucks, H. B. Schlegel *et al.*, Gaussian 09, Revision A.02, Gaussian, Inc., Wallingford, CT, 2009.
- ³⁵C. Adamo and V. Barone, *J. Chem. Phys.* **110**, 6158 (1999).
- ³⁶W. J. Hehre, R. Ditchfield, and J. A. Pople, *J. Chem. Phys.* **56**, 2257 (1972).
- ³⁷P. Hariharan and J. Pople, *Theor. Chim. Acta* **28**, 213 (1973).
- ³⁸J. Riga, J. J. Verbist, F. Wudl, and A. Kruger, *J. Chem. Phys.* **69**, 3221 (1978).
- ³⁹F. P. Cometto, E. M. Patrino, Paredes Olivera, G. Zampieri, and H. Ascolani, *Langmuir* **28**, 13624 (2012).
- ⁴⁰T. Weidner, A. Shaporenko, J. Müller, M. Schmid, P. Cyganik, A. Terfort, and M. Zharnikov, *J. Phys. Chem. C* **112**, 12495 (2008).
- ⁴¹A. Shaporenko, Cyganik, M. Buck, A. Terfort, and M. Zharnikov, *J. Phys. Chem. B* **109**, 13630 (2005).
- ⁴²A. Shaporenko, M. Brunnbauer, A. Terfort, L. S. O. Johansson, M. Grunze, and M. Zharnikov, *Langmuir* **21**, 4370 (2005).
- ⁴³K. Heister, H.-T. Rong, M. Buck, M. Zharnikov, M. Grunze, and L. S. O. Johansson, *J. Phys. Chem. B* **105**, 6888 (2001).
- ⁴⁴G. Heimel, L. Romaner, J.-L. Brédas, and E. Zojer, *Langmuir* **24**, 474 (2008).
- ⁴⁵B. Fiedler, E. Rojo-Wiechel, J. Klassen, J. Simon, J. Beck, and M. Sokolowski, *Surf. Sci.* **606**, 1855 (2012).
- ⁴⁶We note, however, that, for selenolate and thiolate SAMs on Au(111) and Ag(111), marked differences were found for the preferred geometry depending on docking group^{85,86} and metal.^{15,16,40,42,43}
- ⁴⁷Since we do not observe a fixed ratio of IF 1 and IF 2, it is unlikely that only one bonding pattern for all TSeT molecules could explain both selenium interface species.
- ⁴⁸C. D. Zangmeister, L. B. Picraux, R. D. van Zee, Y. Yao, and J. M. Tour, *Chem. Phys. Lett.* **442**, 390 (2007).
- ⁴⁹N. Koch, A. Vollmer, S. Duhm, Y. Sakamoto, and T. Suzuki, *Adv. Mater.* **19**, 112 (2007).
- ⁵⁰H. Yamane, K. Kanai, Y. Ouchi, N. Ueno, and K. Seki, *J. Electron. Spectrosc. Relat. Phenom.* **174**, 28 (2009).
- ⁵¹The (lying) pentacene molecules in these cases have I_{EML}'s of 4.9–5.19 eV,^{49,50,52} and therefore compare slightly better to TSeT than tetracene, whose IE is larger than the one of pentacene by some 100 meV.^{26,87,88}
- ⁵²N. Koch, I. Salzmänn, R. Johnson, J. Pflaum, R. Friedlein, and J. P. Rabe, *Org. Electron.* **7**, 537 (2006).
- ⁵³B. Jaeckel, J. B. Sambur, and B. A. Parkinson, *J. Appl. Phys.* **103**, 063719 (2008).
- ⁵⁴S. Duhm, G. Heimel, I. Salzmänn, H. Glowatzki, R. L. Johnson, A. Vollmer, J. P. Rabe, and N. Koch, *Nat. Mater.* **7**, 326 (2008).
- ⁵⁵S. Duhm, Q. Xin, N. Koch, N. Ueno, and S. Kera, *Org. Electron.* **12**, 903 (2011).
- ⁵⁶N. Koch, *J. Phys. Condens. Matter* **20**, 184008 (2008).
- ⁵⁷H. Yoshida, E. Ito, M. Hara, and N. Sato, *Synth. Met.* **161**, 2549 (2012).
- ⁵⁸E. V. Tsiper, Z. G. Soos, W. Gao, and A. Kahn, *Chem. Phys. Lett.* **360**, 47 (2002).
- ⁵⁹R. Paniago, R. Matzdorf, G. Meister, and A. Goldmann, *Surf. Sci.* **336**, 113 (1995).
- ⁶⁰In a control experiment the initial ϕ was recovered when increasing the temperature back to RT. The ϕ decrease upon cooling is therefore probably related to the adsorption of residual gas molecules, which only stick to

- the surface at low temperatures, and the concomitant push-back effect. The observed decrease of 0.16 eV is well below what was found for a monolayer coverage of xenon (0.5 eV).⁸⁹
- ⁶¹H.-P. Steinrück, *J. Phys. Condens. Matter* **8**, 6465 (1996).
- ⁶²S. Duhm, H. Glowatzki, V. Cimpeanu, J. Klankermayer, J. P. Rabe, R. L. Johnson, and N. Koch, *J. Phys. Chem. B* **110**, 21069 (2006).
- ⁶³M. Schmid, A. Kaftan, H.-P. Steinrück, and J. M. Gottfried, *Surf. Sci.* **606**, 945 (2012).
- ⁶⁴M. G. Betti, A. Kanjilal, C. Mariani, H. Vázquez, Y. J. Dappe, J. Ortega, and F. Flores, *Phys. Rev. Lett.* **100**, 027601 (2008).
- ⁶⁵P. Amsalem, J. Niederhausen, J. Frisch, A. Wilke, B. Bröker, A. Vollmer, R. Rieger, K. Müllen, J. P. Rabe, and N. Koch, *J. Phys. Chem. C* **115**, 17503 (2011).
- ⁶⁶J. Niederhausen, A. Wilke, R. Schlesinger, S. Winkler, A. Vollmer, J. P. Rabe, and N. Koch, *Phys. Rev. B* **86**, 081411 (R) (2012).
- ⁶⁷P. Amsalem, J. Niederhausen, A. Wilke, G. Heimel, R. Schlesinger, S. Winkler, A. Vollmer, J. P. Rabe, and N. Koch, *Phys. Rev. B* **87**, 035440 (2013).
- ⁶⁸S. Braun, W. R. Salaneck, and M. Fahlman, *Adv. Mater.* **21**, 1450 (2009).
- ⁶⁹W. L. Kalb, S. Haas, C. Krellner, T. Mathis, and B. Batlogg, *Phys. Rev. B* **81**, 155315 (2010).
- ⁷⁰C. Krellner, S. Haas, C. Goldmann, K. P. Pernstich, D. J. Gundlach, and B. Batlogg, *Phys. Rev. B* **75**, 245115 (2007).
- ⁷¹For TSeT it was found that the conductivity increases significantly when a vacuum deposited film is heated to 375 K under UHV conditions, which was ascribed to the contact with residual oxygen and the formation of acceptor impurity levels.⁹⁰ We cannot completely rule out the influence of a small fraction of impurities in the present experiments. However, we found that the annealing of TSeT/metal to only slightly above 375 K leads to a drastic change in the valence band spectra for all employed metals. Therefore, the observed decrease in conductivity in Ref. 90 might be a temperature induced effect at the metal contacts.
- ⁷²D. A. Egger, V. G. Ruiz, W. A. Saidi, T. Bucko, A. Tkatchenko, and E. Zojer, *J. Phys. Chem. C* **117**, 3055 (2013).
- ⁷³N. Koch, D. Pop, R. L. Weber, N. Böwering, B. Winter, M. Wick, G. Leising, I. V. Hertel, and W. Braun, *Thin Solid Films* **391**, 81 (2001).
- ⁷⁴C. E. Heiner, J. Dreyer, I. V. Hertel, N. Koch, H.-H. Ritzke, W. Widdra, and B. Winter, *Appl. Phys. Lett.* **87**, 093501 (2005).
- ⁷⁵K. Yokota, M. Taniguchi, and T. Kawai, *J. Am. Chem. Soc.* **129**, 5818 (2007).
- ⁷⁶K. Yokota, M. Taniguchi, and T. Kawai, *J. Phys. Chem. C* **114**, 4044 (2010).
- ⁷⁷N. Sato, H. Inokuchi, and E. A. Silinsh, *Chem. Phys.* **115**, 269 (1987).
- ⁷⁸R. Friedlein, X. Crispin, M. Pickholz, M. Keil, S. Stafström, and W. Salaneck, *Chem. Phys. Lett.* **354**, 389 (2002).
- ⁷⁹F. Bussolotti, S. W. Han, Y. Honda, and R. Friedlein, *Phys. Rev. B* **79**, 245410 (2009).
- ⁸⁰W. Chen, H. Huang, S. Chen, Y. L. Huang, X. Y. Gao, and A. T. S. Wee, *Chem. Mater.* **20**, 7017 (2008).
- ⁸¹G. Heimel, I. Salzmänn, S. Duhm, and N. Koch, *Chem. Mater.* **23**, 359 (2011).
- ⁸²I. Salzmänn, S. Duhm, G. Heimel, M. Oehzelt, R. Kniprath, R. L. Johnson, J. P. Rabe, and N. Koch, *J. Am. Chem. Soc.* **130**, 12870 (2008).
- ⁸³H. Y. Mao, F. Bussolotti, D.-C. Qi, R. Wang, S. Kera, N. Ueno, A. T. S. Wee, and W. Chen, *Org. Electron.* **12**, 534 (2011).
- ⁸⁴F. Bussolotti, S. Kera, K. Kudo, A. Kahn, and N. Ueno, *Phys. Rev. Lett.* **110**, 267602 (2013).
- ⁸⁵D. Käfer, A. Bashir, and G. Witte, *J. Phys. Chem. C* **111**, 10546 (2007).
- ⁸⁶A. Bashir, D. Käfer, J. Müller, C. Wöll, A. Terfort, and G. Witte, *Angew. Chem. Int. Ed.* **47**, 5250 (2008).
- ⁸⁷N. Sato, K. Seki, and H. Inokuchi, *J. Chem. Soc., Faraday Trans. 2* **77**, 1621 (1981).
- ⁸⁸M. L. M. Rocco, M. Haeming, D. R. Batchelor, R. Fink, A. Schöll, and E. Umbach, *J. Chem. Phys.* **129**, 074702 (2008).
- ⁸⁹Y. C. Chen, J. E. Cunningham, and C. P. Flynn, *Phys. Rev. B* **30**, 7317 (1984).
- ⁹⁰I. Shirovani, Y. Kamura, H. Inokuchi, and T. Hirooka, *Chem. Phys. Lett.* **40**, 257 (1976).